DOI: 10.7589/JWD-D-21-00156

Journal of Wildlife Diseases, 58(4), 2022, pp. 926–930

Systemic Infection of *Mycobacterium abscessus* in a Free-Ranging Wild Eurasian Eagle Owl (*Bubo bubo*)

Myeongsu Kim,[1,3,4] Myeon-Sik Yang,[2,4] Jiwon Son,[1,3] Haerin Rhim,[1,3] Tae-Won Jeong,[2] Bumseok Kim,[2] and Jae-Ik-Han[1,3,5] [1]Laboratory of Wildlife Medicine, College of Veterinary Medicine, Jeonbuk National University, Iksan 54596, Republic of Korea; [2]Laboratory of Veterinary Pathology, College of Veterinary Medicine, Jeonbuk National University, Iksan 54596, Republic of Korea; [3]Jeonbuk Wildlife Center, Jeonbuk National University, Iksan 54596, Republic of Korea; [4]These authors contributed equally to this work; [5]Corresponding author (email: jihan@jbnu.ac.kr)

ABSTRACT: An adult Eurasian Eagle Owl (*Bubo bubo*) rescued from drowning was unable to fly. After euthanasia, necropsy and histopathologic examination showed granulomatous inflammation and intracellular acid-fast stain-positive rod-shaped bacteria in the skin, lung, liver, and spleen, which were identified by using molecular analysis as *Mycobacterium abscessus*.

Nontuberculous mycobacteria (NTM) are present in soil and water (Gcebe and Hlokwe 2017). In humans, NTM are known to cause multiple organ infections including pulmonary infection and lymphadenitis (Koh et al. 2013; Johnson and Odell 2014; Lee et al. 2015). In South Africa and Europe, several species of NTM have been isolated from lesions similar to tuberculous lesions in wild animals (García-Jiménez et al. 2015; Gcebe and Hlokwe 2017).

An adult Eurasian Eagle Owl (*Bubo bubo*) was rescued from drowning after it was caught in a net in the Republic of Korea. Initial examination revealed 10% dehydration and low body temperature (<34 C). The wet feathers of the bird were dried, and it was stabilized for a day. On day 2, the bird exhibited inappropriate flight ability in terms of flight distance, height, and posture. Physical examination revealed crackle sounds on inhalation, plus superficial corneal ulcers in both eyes. Radiographic examination, complete blood count, and clinical chemistry revealed no abnormal findings. The bird received intramuscular administration of empirical systemic amoxicillin/clavulanate (Amocla®, Kuhnil Pharm, Seoul, Republic of Korea) and meloxicam (Metacam®, Boehringer Ingelheim, Ingelheim am Phein, Germany) for the possibility of pulmonary infection, and nebulization with a combination of gentamicin (Gentamicin injection®, Shin Poong Pharm, Seoul, Republic of Korea), aminophylline (Aminophylline injection®, Dai Han Pharm, Seoul, Republic of Korea), and acetylcystein (Mucomyst®, Boryung Pharm, Seoul, Republic of Korea) was performed daily. A topical antibiotic and a cell regeneration promoter (Solcoseryl, Solcorin®, Hanrim Pharm, Yongin, Republic of Korea) were instilled for corneal ulcers, and subcutaneous fluid was administered to improve the systemic condition. After 1 wk, dermatitis was observed in the perineum and left carpal joint. Additionally, the left carpal joint showed swelling and bruising. The range of motion of the carpal joint of the left wing was 130–140°. Fine needle aspiration cytology of the left carpal joint revealed granulomatous inflammation in which macrophages were the main inflammatory cells, and a mixed pattern of various bacteria presumed to be caused by lesion contamination. While the bacterial culture of the aspirates was conducted, pentoxifylline (Pentoxin®, Hutecs Pharm, Hwaseong, Republic of Korea) was given in addition to the same antibiotic and nonsteroidal anti-inflammatory drugs. The following day, the skin over the joint was observed to be dry, necrotic, and malodorous; feathers of this area had been shed (Fig. 1a). Subsequently, the range of motion worsened (110°). The next day, most of the original lesions had turned necrotic and developed a foul odor, and similar lesions were identified near the left ulna. Euthanasia was carried out because of the poor prognosis for survival in the wild.

Necropsy revealed ulceration and necrosis of the skin in the left carpal joint area (Fig. 1b). A solid mass of approximately 1.5 cm diameter was observed within the skin lesion. Unexpectedly, necropsy revealed fibro-puru-

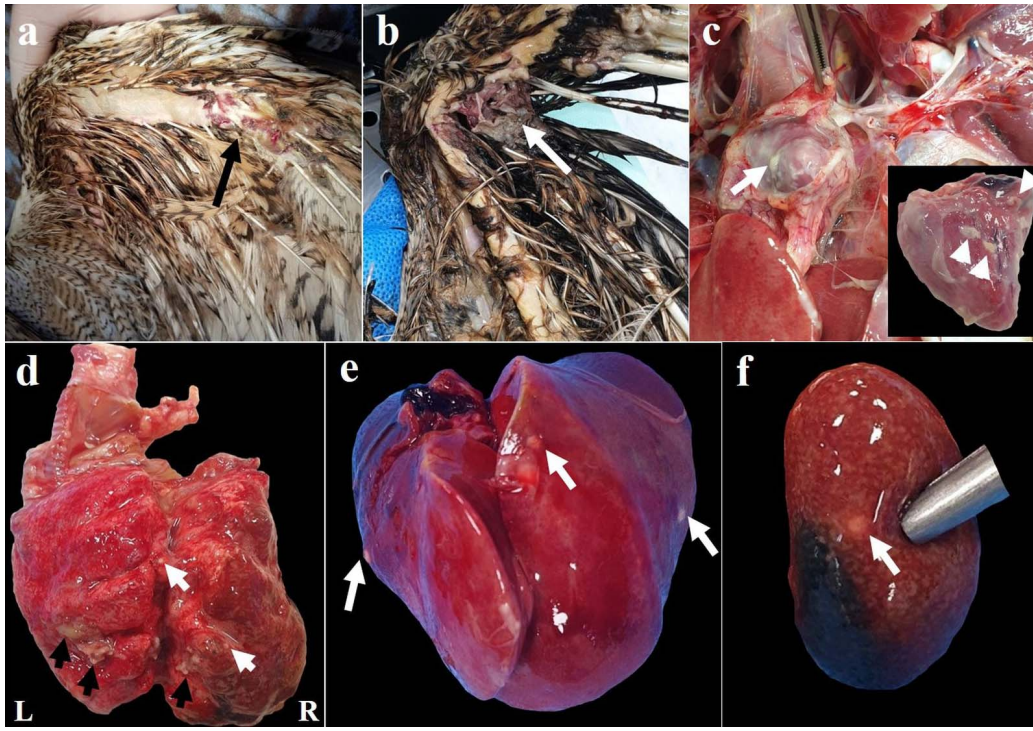

FIGURE 1. Physical examination and necropsy findings in an adult Eurasian Eagle Owl (*Bubo bubo*) admitted for rehabilitation in the Republic of Korea. (a) Dry, necrotic, and malodorous skin lesion of the left carpal area (black arrow). (b) Left carpal joint; skin ulceration and necrosis (white arrow). (c) Heart; fibro-purulent pericardial effusion and debris attachment (white arrows). Inset: Heart. (d) Lung; multifocal white nodules <1 mm diameter (white arrows) and fibro-purulent deposition (black arrows). (e) Liver and (f) spleen; multifocal white nodules <1 mm diameter (white arrows).

lent exudates filling the pericardial space and attached to the epicardium (Fig. 1c). Small numbers of multifocal white nodules (less than 1 mm diameter) and fibro-purulent debris were observed in the lung tissue (Fig. 1d). A few multifocal white nodules (less than 1 mm) were observed in the liver and spleen (Fig. 1e, f). Histopathologically, the skin showed acanthosis and caseous necrosis in the epidermis. In some areas, a pseudomembrane composed of mononuclear inflammatory cells and fibrinous exudate was formed and covered the epidermis. Numerous degenerated inflammatory cells were accumulated in the epidermis. Acid-fast bacteria were detected in the pseudomembrane (Fig. 2a). The solid mass found in the carpal joint showed caseous necrotic changes, and mononuclear inflammatory cells were infiltrated into the mass. Variable sizes of canal were observed inside the mass. The margins of the canals were composed of necrotic cellular debris; acid-fast bacteria were detected throughout the mass, especially at the canal margins (Fig. 2b). Granulomas of various sizes were observed in the heart, lung, liver, and spleen, and were composed of a central caseous necrotic area and peripheral multinucleated giant cells (Fig. 2c, d). Using Ziehl-Neelsen stain, acid-fast bacilli were detected throughout the granulomas. The multinucleated giant cells had an atypical shape, and vacuolar structures with various sizes were observed inside. Acid-fast positive reactions were observed both in multinucleated giant cells and in peripheral mononuclear inflammatory cells. On the outside of the multinucleated giant cell zone, mononuclear inflammatory cells formed a border and encapsulated the granuloma (Fig. 2c, d). Within some of giant cells,

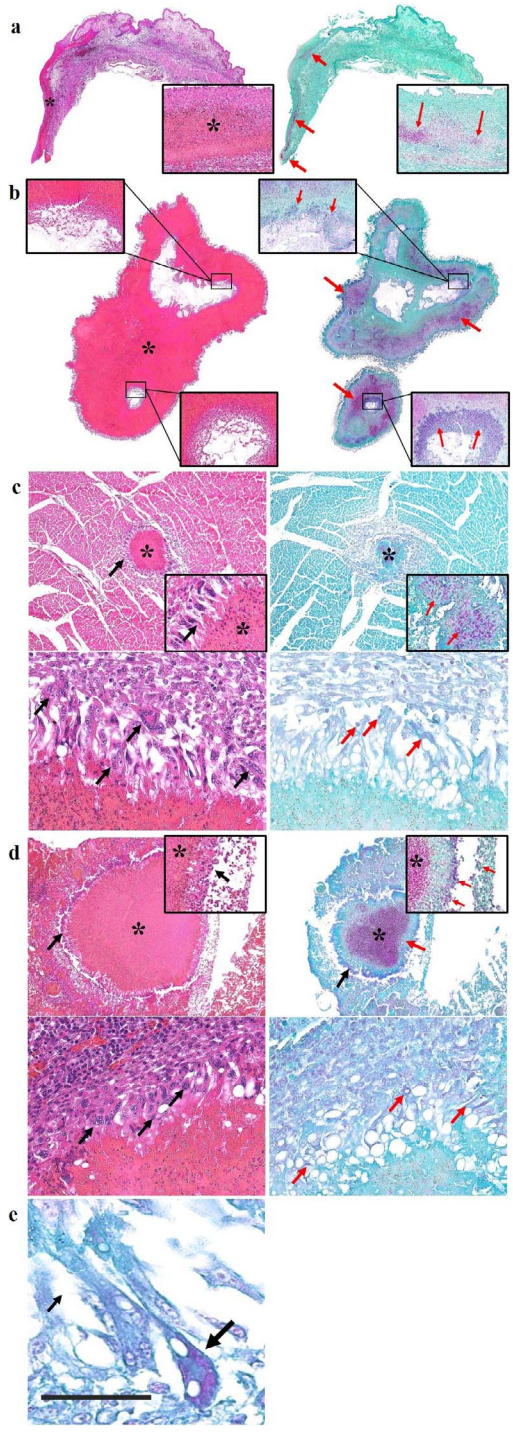

FIGURE 2. Histologic findings in an adult Eurasian Eagle Owl (*Bubo bubo*) admitted for rehabilitation in the Republic of Korea. H&E (left) and acid-fast (right, counterstain with methyl green) staining. (a) Skin on the left carpal area. Acanthosis, caseous necrosis, and pseudomembrane (asterisks) in the epidermis. Acid-fast stain positive cells (red arrows) are seen in the epidermis. (b) Solid neoplasm on the left carpal area. Caseous necrosis (asterisk) and acid-fast stain positive cells (red arrows). Insert: higher magnification. Granulomas with central caseous necrosis (asterisks), peripheral multinucleated giant cells (black arrows), and acid-fast stain positive cells (red arrows) in the (c) heart and (d) lung; insets show higher magnification. (e) Acid-fast positive giant cell (black arrow). Bar=20 μm.

aggregated acid-fast bacteria were observed (Fig. 2e). Acid-fast rod-shaped bacilli also were observed in lung parenchyma and inside granulomas (Supplementary Material Fig. S1a, b).

We performed molecular analyses for bacterial identification. Genomic DNA was extracted from the skin, heart, lung, liver, and spleen using a QIAamp® DNA Mini kit (Qiagen, Hilden, Germany). The PCR amplification was performed with primers 16SRNAF and 16SRNAR for the mycobacterial *16S rRNA* gene, as described (Huard et al. 2003). Similarly, the *rpo*B gene was amplified using the primers MycoF and MycoR, as described (Adékambi et al. 2003). Compared to the sequences in the GenBank database, the *16S rRNA* gene sequence was identified as *Mycobacterium* sp. (GenBank accession no. AP018436). Because the sequence of the *rpoB* gene was 100% identical to that of *M. abscessus* (GenBank accession no. JF346872), and considering all the relevant information, the patient was finally diagnosed with systemic NTM infection (Fig. 3).

Mycobacterium abscessus is a part of a group of environmental mycobacteria related to those that cause tuberculosis and leprosy (Franco-Paredes et al. 2018). In wild animals, *M. abscessus* infection has been reported in lions (*Panthera leo*), hyenas (*Crocuta crocuta*), and leopards (*Panthera pardus*) (Gcebe and Hlokwe 2017) but not in birds. In humans, *M. abscessus* is included in a group of rapidly growing mycobacteria that are responsible for infection of the skin and internal organs (Lee et al. 2015). A human skin infection has been described with *M. chelonae/abscessus* infec-

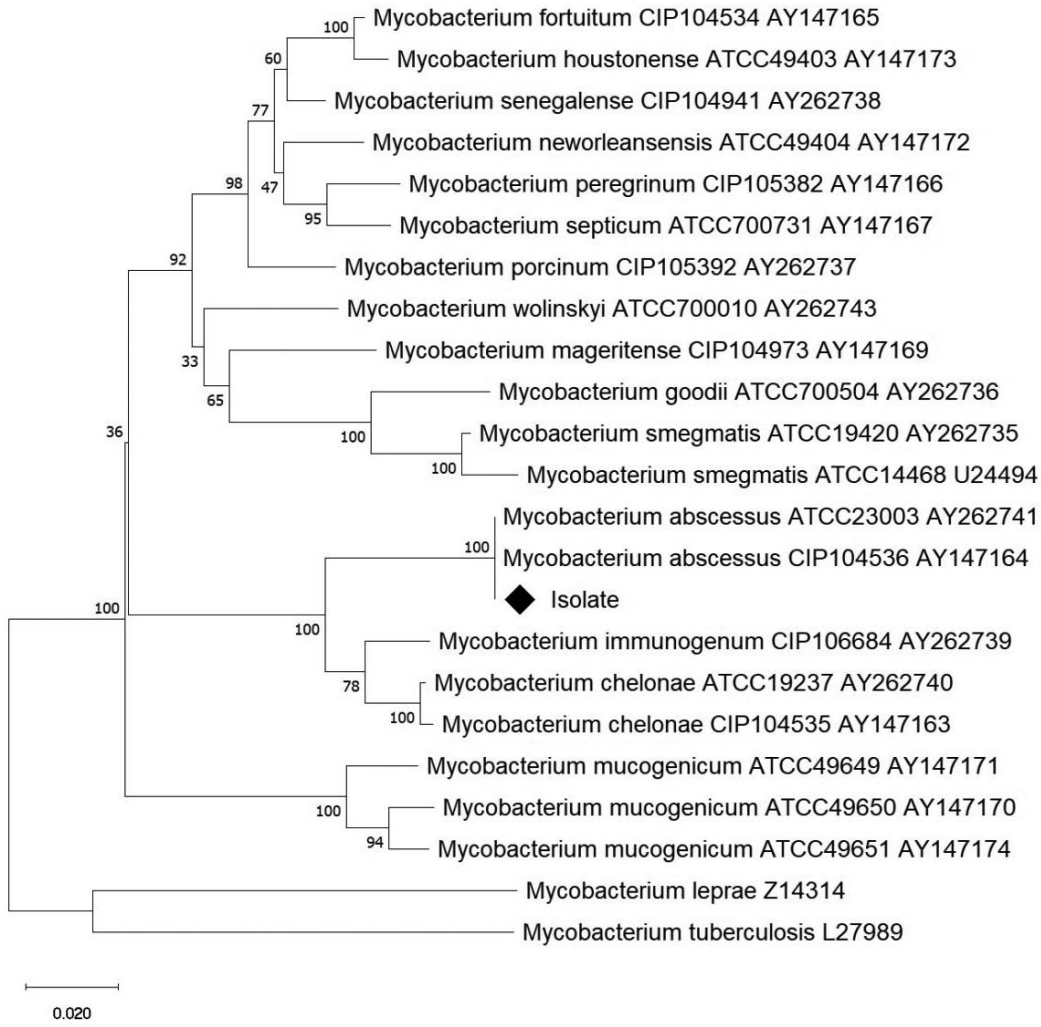

FIGURE 3. Neighbor-joining phylogenetic analysis based on the partial *rpoB* gene sequences in the GenBank databases. Diamond indicates *Mycobacterium abscessus* identified in the Eurasian Eagle Owl (Bubo bubo) in this study. Sequence alignments were performed using ClustalX version 1.8 (Thompson et al. 1997); MEGA-X version 10.1 (Kumar et al. 2018) was used for phylogenetic analyses. Bootstrap percentage values are shown on the branches.

tion at the site of a bite by a pet cockatoo, indicating the possibility that the bird might have been a transmitter of the mycobacteria (Larson et al. 2008). Once the infection is established, *M. abscessus* forms granulomas, which help the bacteria to resist the immune system (Johansen et al. 2020). In our case, the owl was initially suspected to have a simple infection limited to the skin, but necropsy revealed widespread infection of the internal organs, suggesting that the infection might have become established before the rescue. Mycobacterial pathogenic factors, and the fact that the bird was caught in a fishing net for quite some time and restricted in a small cage during hospitalization, might have caused immunosuppression. This could have triggered the rapid collateral spread of mycobacterial infection to the skin.

This publication was supported by the National Institute of Wildlife Disease Control and Prevention as "Specialized Graduate School Support Project for Wildlife Disease Specialists."

SUPPLEMENTARY MATERIAL

Supplementary material for this article is online at http://dx.doi.org/10.7589/JWD-D-21-00156.

LITERATURE CITED

Adékambi T, Colson P, Drancourt M. 2003. *rpo*B-based identification of nonpigmented and late-pigmenting rapidly growing mycobacteria. *J Clin Microbiol* 41: 5699–5708.

Franco-Paredes C, Marcos LA, Henao-Martínez AF, Rodríguez-Morales AJ, Villamil-Gómez WE, Gotuzzo E, Bonifaz A. 2018. Cutaneous mycobacterial infections. *Clin Microbiol Rev* 32:e00069–18.

García-Jiménez WL, Benítez-Medina JM, Martínez R, Carranza J, Cerrato R, García-Sánchez A, Risco D, Moreno JC, Sequeda M, et al. 2015. Non-tuberculous mycobacteria in wild boar (*Sus scrofa*) from southern Spain: Epidemiological, clinical and diagnostic concerns. *Transbound Emerg Dis* 62:72–80.

Gcebe N, Hlokwe TM. 2017. Non-tuberculous mycobacteria in South African wildlife: Neglected pathogens and potential impediments for bovine tuberculosis diagnosis. *Front Cell Infect Microbiol* 7:15.

Huard RC, de Oliveira Lazzarini LC, Butler WR, van Soolingen D, Ho JL. 2003. PCR-based method to differentiate the subspecies of the *Mycobacterium tuberculosis* complex on the basis of genomic deletions. *J Clin Microbiol* 41:1637–1650.

Johansen MD, Herrmann JL, Kremer L. 2020. Non-tuberculous mycobacteria and the rise of *Mycobacterium abscessus*. *Nat Rev Microbiol* 18:392–407.

Johnson MM, Odell JA. 2014. Nontuberculous mycobacterial pulmonary infections. *J Thorac Dis* 6:210–220.

Koh W-J, Chang B, Jeong B-H, Jeon K, Kim S-Y, Lee NY, Ki C-S, Kwon OJ. 2013. Increasing recovery of nontuberculous mycobacteria from respiratory specimens over a 10-year period in a tertiary referral hospital in South Korea. *Tuberc Respir Dis (Seoul)* 75:199–204.

Kumar S, Stecher G, Li M, Knyaz C, Tamura K. 2018. MEGA X: Molecular evolutionary genetics analysis across computing platforms. *Mol Biol Evol* 35:1547–1549.

Larson JM, Gerlach SY, Blair JE, Brumble L, Jorn HK, Thompson JM. 2008. *Mycobacterium chelonae/abscessus* infection caused by a bird bite. *Inf Dis Clin Prac* 16:60–61.

Lee MR, Sheng WH, Hung CC, Yu CJ, Lee LN, Hsueh PR. 2015. *Mycobacterium abscessus* complex infection in humans. *Emerg Infect Dis* 21:1638–1646.

Thompson JD, Gibson TJ, Plewniak F, Jeanmougin F, Higgins DG. 1997. The CLUSTAL_X windows interface: Flexible strategies for multiple sequence alignment aided by quality analysis tools. *Nucleic Acids Res* 25:4876–4882.

Submitted for publication 22 September 2021.
Accepted 21 June 2022.